Journal of Alloys and Compounds 509 (2011) 8333–8336

Contents lists available at ScienceDirect

Journal of Alloys and Compounds

journal homepage: www.elsevier.com/locate/jallcom

Rapidly directional solidification of highly undercooled Ni–Fe–Ga shape memory alloy melts

Hongxing Zheng[a,b,*], Sichuang Xue[a,b], Dianzhen Wu[a,b], Qijie Zhai[b]

[a] Laboratory for Microstructures, Shanghai University, Shanghai 200444, China
[b] Shanghai Key Laboratory of Modern Metallurgy and Materials Processing, Shanghai University, Shanghai 200072, China

ARTICLE INFO

Article history:
Received 6 April 2011
Received in revised form 3 June 2011
Accepted 6 June 2011
Available online 16 June 2011

Keywords:
Ni–Fe–Ga
Directional solidification
Martensitic transformation
High undercooling

ABSTRACT

In the present work, high undercooling rapid solidification technique is applied to the directional crystal growth of ternary Ni–Fe–Ga shape memory alloys (SMAs). Experimental results show that the phase selection of undercooled melts strongly depends on the triggering mode and nucleation undercooling. With the planar triggering nucleation at the undercooling of 160 K from the bottom of alloy melt, a directionally solidified sample with a preferred (2 0 0) orientation of γ phase is obtained. When the point triggering mode is employed at 180 K, γ phase is suppressed completely and the directionally solidified sample demonstrates almost identical phase transformation temperatures.

1. Introduction

Shape memory alloys (SMAs) are used in a wide range of applications including actuators, sensors, vibration dampers, underwater sound projectors and surface control systems [1,2]. In traditional SMAs, which are paramagnetic, the martensitic transformation underlying the shape memory effect (SME) is induced by means of changes in either temperature or stress or both. Traditional SMAs, such as NiTi, Cu- and Fe-based alloys, are capable of providing high strains, but they are actuated by heating or cooling, which is relatively slow [3–6]. On the other hand, the same transformation in ferromagnetic shape memory alloys (FSMAs) can be triggered not only by changes in temperature and stress, but also by changes in the applied magnetic field. Compared with traditional SMAs driven by temperature, FSMAs show large output strains, a high impetus and short response times (below 1 ms) induced by the magnetic field and therefore, it is expected that FSMAs would have wider applicability. So far, among many FSMAs such as Ni–Mn–Ga, Fe–Pt, Co–Ni and Fe–Ni–Co–Ti, Heusler alloys are the most promising demonstrating up to 9.5% magnetic-field-induced strain (MFIS) in an applied field [7–9]. Subsequently, some new Heusler alloys, such as Ni–Fe–Ga, Ni–Mn–Fe–Ga, Co–Ni–Ga and Co–Ni–Al were explored. These Heusler alloys, with a reversible martensitic transformation, also possess the capability of magnetic-field-induced strain which can also be used to produce thermal SMAs with a narrow hysterisis (less than 10 K) [10–14].

For Heusler FSMAs, the conventional synthesis is arc-melting followed by annealing at a specific temperature to achieve a structural transition from B2 to $L2_1$. It has been thought to be an effective way to improve the properties by fabricating materials with preferred orientations because of strong anisotropy for those kinds of functional materials. Some work on the fabrication of directional materials has been conducted [15–17]. The main problem is the difficulty to control the composition homogeneity along the rod axis. Recently a new approach through high undercooling rapid solidification technique has been proposed and applied successfully in Fe–Ga and Co–Ni–Ga materials [18,19]. In the present work, directional solidification of ternary Ni–Fe–Ga alloys are performed with the application of high undercooling technique and the phase selection characteristics of directionally solidified Ni–Fe–Ga alloy under two different triggering nucleation modes are investigated to provide more information for the development of this innovative materials preparation technique.

2. Experimental procedures

$Ni_{56.3}Fe_{17}Ga_{26.7}$ (at.%) ingot was prepared using conventional arc melting from Ni, Fe, Ga with purities of 99.99 wt.% under argon atmosphere. The ingot was then injected into a cylindrical chilled copper mold to fabricate a rod with a dimension of 7 mm in diameter and 80 mm in length, which is cut in half for the following undercooling experiments. The schematic set-up of high undercooling directional crystal growth is shown in Fig. 1. Firstly, the alloy rod was put into the quartz tube (7 mm in diameter and 50 mm in height) with inorganic glass purifier covered on the surface. The inorganic glass (50 wt.%B_2O_3 + 30 wt.%Na_2SiO_3 + 20 wt.%$Na_2B_4O_7$) used as denucleating agent [18]. The alloy was induction melted and the glass purifier coated

* Corresponding author at: Laboratory for Microstructures, Shanghai University, Shanghai 200444, China. Tel.: +86 21 56331218; fax: +86 21 56331218.
E-mail address: hxzheng@shu.edu.cn (H. Zheng).

0925-8388/$ – see front matter © 2011 Elsevier B.V. All rights reserved.
doi:10.1016/j.jallcom.2011.06.023

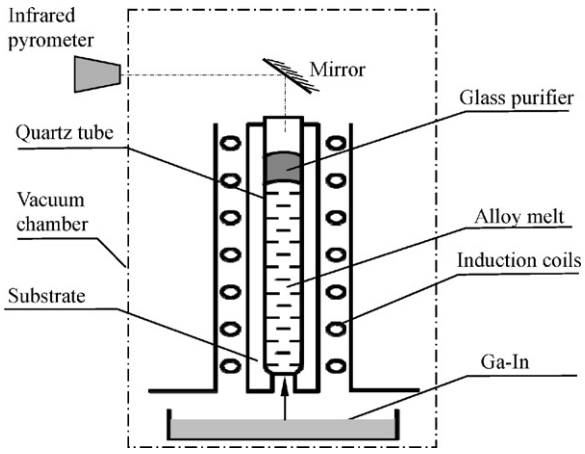

Fig. 1. Schematic diagram of high undercooling directional crystal growth set-up.

the surface of the sample to purify the alloy melt. The temperature was monitored through an infrared sensing system with an absolute accuracy better than ±10 K and a response time less than 5 ms. Once the undercooling reached the preset value, the quartz tube dropped down to contact the Ga–In cooling media quickly (the melting point of 75%Ga25%In (wt.%) used in the present study is about 289 K) and nucleation was triggered. The alloy melting point was measured in a differential thermal analysis (DTA1600) to further calibrate the temperature of cooling curves. In the present work, the contact surface of quartz tube bottom (black arrow pointing up in Fig. 1) was designed to two different shapes, one is planar and the other is spherical to simulate different nucleation modes, planar triggering and point triggering, respectively. The directionally solidified samples obtained (7 mm in diameter and ~35 mm in height) were annealed at 773 K for 30 min.

The orientation along the growth direction of directionally solidified samples was characterized by X-ray diffraction (DLMAX-2550) using CuKα radiation. Microstructural observation was conducted using an optical microscope and a scanning electron microscope (JSM-6700F). Differential scanning calorimetry (NETZSCH DSC 204 F1) measurements were carried out to examine the characteristic temperatures of martensitic transformation with heating/cooling rates of 10 K/min.

3. Results and discussion

When the $Ni_{56.3}Fe_{17}Ga_{26.7}$ alloy melt was undercooled to the nucleation temperature, T_N, nucleation abruptly and growth occurred. The temperature would rise quickly to the recalescence temperature, T_R, due to the latent heat released by the primary solidified solid phase. After this recalescence, the sample cooled down slowly. The melting point of $Ni_{56.3}Fe_{17}Ga_{26.7}$ alloy is about

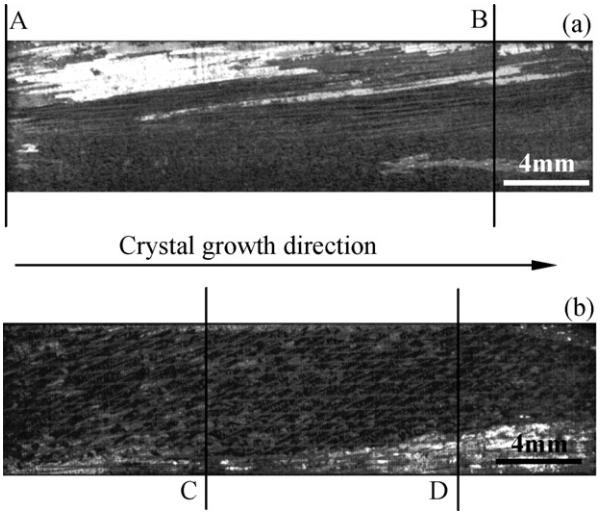

Fig. 2. Macrostructures of directionally solidified $Ni_{56.3}Fe_{17}Ga_{26.7}$ sample I, planar triggering at the undercooling of 160 K (a) and sample II, point triggering at 180 K (b).

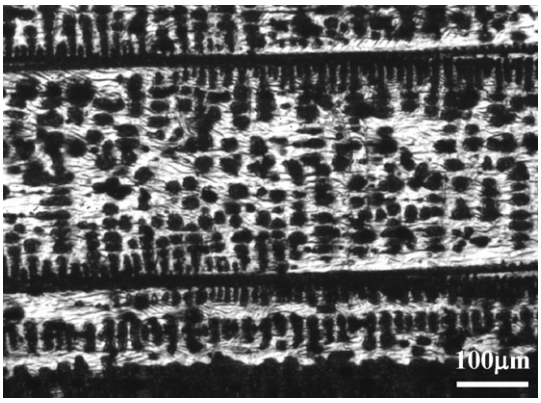

Fig. 3. Microstructure of directionally solidified sample I.

1532 K (DTA result not shown here). Fig. 2 gives the macrostructures of directionally solidified samples obtained under different conditions. The upper one is prepared with planar triggering mode from the bottom of melt under the undercooling of 160 K (the nucleation temperature of the alloy is 1372 K). The lower one is obtained with point triggering at 180 K (T_N = 1352 K). One can observe clear features of directional growth from left to right in Fig. 2 (hereinafter referred to as "sample I" and "sample II", respectively).

In case of sample I, the microstructure is presented in Fig. 3 where the sample is taken along the growth direction. Black γ phase grows in the form of dendrites paralleled to the rod axis and some γ particles distributed in the white matrix, which is confirmed to be martensitic phase with a tetragonal structure at room temperature transformed from high temperature austenite phase based on the XRD pattern (Fig. 4). The XRD pattern of arc-melted master alloy indicates that only one weak (2 0 0) peak of γ phase is detected and the master alloy is mainly composed of martensitic phase. However, a strong (2 0 0) orientation of γ phase appears at the initial directional solidification stage (location A marked in Fig. 2a) and when the crystal grows to the location B, the orientation becomes weak although γ phase is still the main skeleton phase.

In case of sample II, the macrostructure of nucleation site taken from the bottom reveals a few large grains formed with the nucleation occurring (Fig. 5a). Fig. 5b is the microstructure of sample II with typical plate-like martensitic phase, no visible γ phase is found. DSC charts from locations C and D marked in Fig. 2b demonstrate almost identical phase transformation temperatures (Fig. 6).

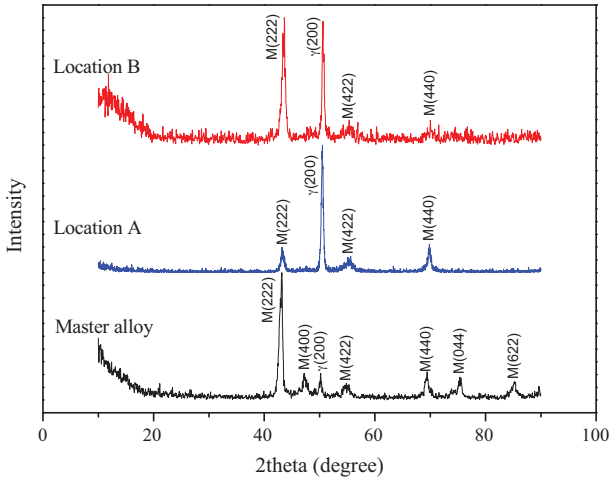

Fig. 4. XRD patterns of master alloy and directionally solidified sample I from locations A and B marked in Fig. 2a.

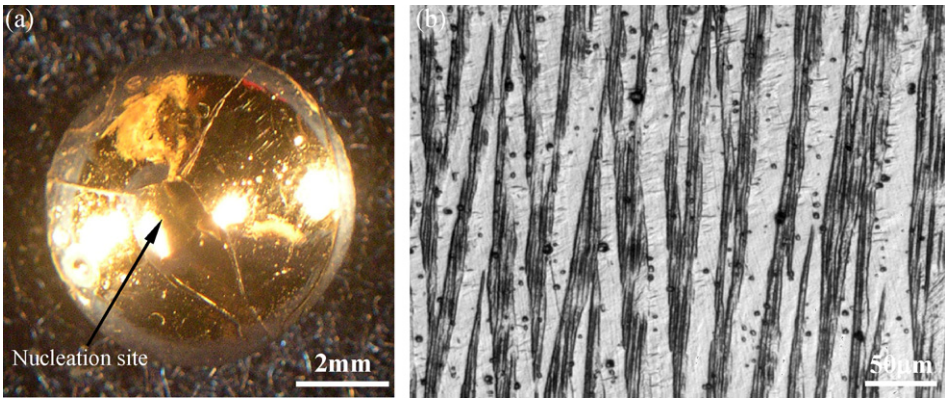

Fig. 5. Macrostructure of nucleation site (a) and microstructure (b) of directionally solidified sample II.

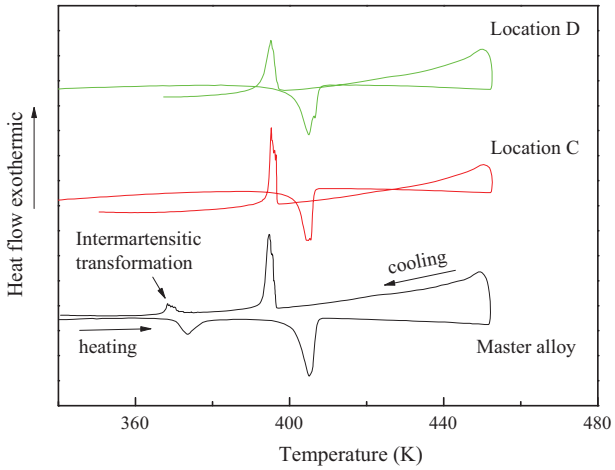

Fig. 6. DSC charts of master alloy and directionally solidified sample II from locations C and D marked in Fig. 2b.

Compared with the arc-melted master alloy, the intermartensitic transformation that occurs in the vicinity of 370 K disappears in the undercooled directional solidified sample II. However, the martensitic transformation temperatures almost coincides with that of master alloy implying the compositions do not change before and after high undercooling cycles. Meanwhile, considering the transformation temperatures are highly sensitive to the compositions, it is concluded that the compositions are very homogeneous along the rod axis.

Generally speaking, the difference of Gibbs energy caused by high undercooling near the solid/liquid interface acts as the driving force to push the crystal grow quickly for undercooled melt. Once the crystal begins to grow, it is inevitable to release latent heat, which would result in a continuous decrease of interface undercooling. In other words, the driving force decreases with the occurrence of crystal growth and at the end stage, the driving force is not enough, thus other phases or grains with other orientations may appear. This is why the orientation of γ phase weakens and more austenite forms at the end stage for the sample I. On the other hand, it is also reasonable to conclude that the latent heat would remelt part of γ primary dendritic phase and result in the formation of some interdendritic γ particles. With the completion of rapid solidification, residual austenitic phase begins to solidify between the primary γ dendritic skeletons.

However, one cannot observe γ phase in the sample II which can be explained by the absence of "quenching effect". Even though sample I nucleates at the nominal thermodynamic undercooling of 160 K, a large dynamic undercooling may be introduced by the application of planar triggering, that is so called "quenching effect", which would lead to the effective undercooling higher than 160 K. With the contribution of quenching effect, γ phase becomes the primary phase formed during the rapid solidification instead of austenitic phase. However, in the case of sample II, the point triggering does not introduce serious dynamic undercooling. Consequently, although the nucleation undercooling of 180 K is slightly higher than that of sample I (160 K), γ phase is still suppressed completely and a fully austenite is obtained.

As discussed above, the interface undercooling decreases continuously with the crystal growth because of the release of latent heat, however, the DSC results obtained at different locations from sample II reveals that the nucleation undercooling does not have any effect on the transformation temperatures after annealing at 773 K for 30 min, this is in agreement with our previous report [20]. Li et al. [19] fabricated Co–Ni–Ga unidirectional crystal using similar technique and found that the transformation temperatures enhanced for the undercooled single crystal and they ascribed to the large internal stress caused by the nature of rapid solidification. The appearance of some small black cavities in sample II (Fig. 5b) also supports this point. Therefore, from the viewpoint of engineering applications, the undercooled directionally solidified SMA materials need to release the residual internal stress in order to gain homogeneous phase transformation temperatures along the rod axis.

4. Conclusions

In summary, high undercooling rapid solidification technique is an effective and feasible approach to fabricate directional Ni–Fe–Ga shape memory alloys. However, the phase selection of undercooled melts strongly depends on the nucleation triggering mode and nucleation undercooling. Further work is required to be done to clarify the effects of those two factors for the development of this innovative materials preparation technique.

Acknowledgements

All the authors gratefully acknowledge the financial support from the Shanghai Pujiang Program (10PJ1404200) and the Innovative Program of Shanghai University of China. Hongxing Zheng acknowledges funding from the Alexander von Humboldt (AvH) Foundation of Germany.

References

[1] K. Ullakko, J. Mater. Eng. Perform. 5 (1996) 405.
[2] O. Heczko, N. Glavatska, V. Gavriljuk, K. Ullakko, Mater. Sci. Forum 373-376 (2001) 341.

[3] L.E. Kozlova, A.N. Titenko, Mater. Sci. Eng. A 438-440 (2006) 738.
[4] H.X. Zheng, J. Mentz, M. Bram, et al., J. Alloys Compd. 463 (2008) 250.
[5] S. Kajiwara, Mater. Sci. Eng. A 273-275 (1999) 67.
[6] B. Kockar, I. Karaman, J.I. Kim, et al., Acta Mater. 56 (14) (2008) 3630.
[7] K. Oikawa, T. Ota, F. Gejima, et al., Mater. Trans. 42 (2001) 2472.
[8] I. Karaman, H.E. Karaca, D.C. Lagoudas, et al., Scripta Mater. 49 (2003) 831.
[9] K. Oikawa, T. Ota, Y. Sutou, et al., Mater. Trans. 43 (2002) 2360.
[10] H.X. Zheng, M.X. Xia, J. Liu, et al., Acta Mater. 53 (19) (2005) 5125.
[11] J. Liu, N. Scheerbaum, D. Hinz, O. Gutfleisch, Acta Mater. 56 (13) (2008) 3177.
[12] A.A. Cherechukin, V.V. Khovailo, R.V. Koposov, et al., J. Magn. Magn. Mater. 258-289 (2003) 523.
[13] I. Glavatskyy, N. Glavatska, I. Urubkov, et al., Mater. Sci. Eng. A 481-482 (2008) 298.
[14] H.E. Karaca, I. Karaman, Y.I. Chumlyakov, et al., Scripta Mater. 51 (3) (2004) 261.
[15] H.X. Zheng, W.Z. Ma, Y.Y. Lu, et al., J. Mater. Sci. 39 (7) (2004) 2557.
[16] D.L. Schlagel, Y.L. Wu, W. Zhang, T.A. Lograsso, J. Alloys Compd. 321 (2000) 77.
[17] T. Liang, C.B. Jiang, H.B. Xu, et al., J. Magn. Magn. Mater. 268 (2004) 29.
[18] W.Z. Ma, H.X. Zheng, M.X. Xia, J.G. Li, J. Alloys Compd. 379 (1–2) (2004) 188.
[19] J.Z. Li, J. liu, J.G. Li, J. Alloys Compd. 509 (2011) 6777.
[20] H.X. Zheng, M.X. Xia, J. Liu, J.G. Li, J. Alloys Compd. 388 (2) (2005) 172.